Slb/Wnt11 controls hypoblast cell migration and morphogenesis at the onset of zebrafish gastrulation

Florian Ulrich[1,*], Miguel L. Concha[2,3,*], Paul J. Heid[4], Ed Voss[4], Sabine Witzel[1], Henry Roehl[5], Masazumi Tada[2], Stephen W. Wilson[2], Richard J. Adams[6], David R. Soll[4] and Carl-Philipp Heisenberg[1,†]

[1]Max Planck Institute of Molecular Cell Biology and Genetics, Pfotenhauerstrasse 108, 01307 Dresden, Germany
[2]University College London, Department of Anatomy and Developmental Biology, Gower Street, London WC1E 6BT, UK
[3]Programa de Morfologia, Instituto de Ciencias Biomedicas, Facultad de Medicina, Universidad de Chile, PO Box 70079, Santiago de Chile, Chile
[4]University of Iowa, Department of Biological Sciences, Iowa City, IA 52242, USA
[5]Max-Planck-Institut für Entwicklungsbiologie, Spemannstrasse 35 / III, 72076 Tübingen, Germany
[6]University of Cambridge, Department of Anatomy, Downing Street, Cambridge CB2 3DY, UK
*These authors contributed equally to this work
†Author for correspondence (e-mail: heisenberg@mpi-cbg.de)

Accepted 21 July 2003

Development 130, 5375-5384
© 2003 The Company of Biologists Ltd
doi:10.1242/dev.00758

Summary

During vertebrate gastrulation, highly coordinated cellular rearrangements lead to the formation of the three germ layers, ectoderm, mesoderm and endoderm. In zebrafish, *silberblick* (*slb*)*/wnt11* regulates normal gastrulation movements by activating a signalling pathway similar to the Frizzled-signalling pathway, which establishes epithelial planar cell polarity (PCP) in *Drosophila*. However, the cellular mechanisms by which *slb/wnt11* functions during zebrafish gastrulation are still unclear. Using high-resolution two-photon confocal imaging followed by computer-assisted reconstruction and motion analysis, we have analysed the movement and morphology of individual cells in three dimensions during the course of gastrulation. We show that in *slb*-mutant embryos, hypoblast cells within the forming germ ring have slower, less directed migratory movements at the onset of gastrulation. These aberrant cell movements are accompanied by defects in the orientation of cellular processes along the individual movement directions of these cells. We conclude that *slb/wnt11*-mediated orientation of cellular processes plays a role in facilitating and stabilising movements of hypoblast cells in the germ ring, thereby pointing at a novel function of the *slb/wnt11* signalling pathway for the regulation of migratory cell movements at early stages of gastrulation.

Movies available online

Key words: Wnt signalling, Cell migration, Gastrulation, Zebrafish

Introduction

Cell polarity and directed cell migration are essential components that underlie tissue morphogenesis in several developmental processes. During vertebrate gastrulation, a seemingly unstructured blastula transforms into a gastrula with distinct populations of cells organised into the three germ layers, ectoderm, mesoderm and endoderm. The different types of cell movements that underlie these cellular rearrangements are best studied in the amphibian *Xenopus* (reviewed by Keller et al., 2000). Involution or ingression of prospective mesendodermal cells at the onset of gastrulation is followed by convergence and extension movements of mesendodermal and ectodermal cells, which is commonly termed convergent extension (CE) (Elul et al., 1997; Keller and Danilchik, 1988; Keller et al., 1985). In CE, cells move towards the dorsal side of the gastrula where they undergo medio-lateral cell intercalations that lead to a medio-lateral narrowing and anterior-posterior extension of the forming body axis (Keller and Tibbetts, 1989; Shih and Keller, 1992). CE movements are usually accompanied by an elongation of cells along their medio-lateral axis, but it is not clear if this is a consequence of or prerequisite for CE movements (Elul and Keller, 2000; Keller et al., 1992).

The molecular basis underlying cell movements during vertebrate gastrulation is only beginning to be unravelled. Several studies have shown that Wnt genes are important for normal gastrulation movements, both in *Xenopus* and in zebrafish (reviewed by Keller, 2002; Tada et al., 2002; Wallingford et al., 2002). The signalling pathway through which these Wnt ligands transmit their morphogenetic activity shares several components with the Frizzled (Fz) signalling cascade involved in the establishment of epithelial PCP in *Drosophila*. Such shared components include the Wnt receptor Frizzled (Fz), the intracellular signalling mediator Dishevelled (Dsh), the small GTPases RhoA, Rac and Cdc42, the Rho effector Rho Kinase 2 (Rok2), the transmembrane protein Strabismus/van Gogh (Stbm/Vang) and the β′ subunit of Protein Phosphatase 2A (PP2A), Widerborst (Wdb) (Darken et al., 2002; Djiane et al., 2000; Goto and Keller, 2002; Habas et al., 2001; Habas et al., 2003; Hannus et al., 2002; Heisenberg et al., 2000; Marlow et al., 2002; Park and Moon, 2002; Sumanas and Ekker, 2001; Sumanas et al., 2001; Wallingford et al., 2000).

In zebrafish, several mutants that exhibit defects in cell movements during gastrulation have been identified. In *pipetail* (*ppt*)/*wnt5*, *knypek* (*kny*)/*glypican4/6* and *trilobite* (*tri*)/*stbm* mutants, CE movements are predominantly affected in posterior regions of the gastrula, whereas in *slb/wnt11* (*slb*) embryos, CE movements in both anterior and posterior parts of the gastrula are defective (Hammerschmidt et al., 1996; Heisenberg et al., 2000; Jessen et al., 2002; Kilian et al., 2003; Rauch et al., 1997; Solnica-Krezel et al., 1996; Topczewski et al., 2001). Epistasis experiments indicate that *kny/glypican4/6* can function in the *slb/wnt11* signalling pathway, whereas *tri/stbm* appears to act in a parallel pathway (Heisenberg and Nüsslein-Volhard, 1997; Topczewski et al., 2001). However, the way in which these genes regulate gastrulation movements on a cellular basis is not yet fully understood.

Comparison of the functions of the Wnt/PCP pathway during vertebrate gastrulation and the Fz/PCP pathway in *Drosophila* reveals conserved and divergent signalling mechanisms. In the *Drosophila* wing disc, the Fz/PCP pathway determines polarity of cells along the proximal-distal axis, which results in the directed outgrowth of a single wing hair at the distal tip of those cells (reviewed by Adler, 2002). Proximal-distal cell polarization is preceded by an asymmetric localization of various components of the PCP pathway, such as Fz, Dsh, Fmi, Diego and Wdb, to the proximal and/or distal cortical domains of these cells (reviewed by Strutt, 2002). During vertebrate gastrulation, components of the Wnt/PCP pathway, such as Dsh and Stbm/Vang, are localised to the cell membrane (Park and Moon, 2002; Wallingford et al., 2000). However, no asymmetric distribution of these proteins has been observed. Morphologically, ectodermal and mesendodermal cells undergoing CE movements are elongated along their medio-lateral axis at late stages of gastrulation (Concha and Adams, 1998; Elul and Keller, 2000; Keller et al., 1992). Several studies in *Xenopus* and zebrafish demonstrate that the medio-lateral elongation of these cells is regulated by components of the Wnt/PCP pathway such as Dsh, Kny/Glypican4/6, Tri/Stbm, Rok2 and Ppt/Wnt5 (Darken et al., 2002; Goto and Keller, 2002; Jessen et al., 2002; Kilian et al., 2003; Marlow et al., 2002; Topczewski et al., 2001; Wallingford et al., 2000). Thus, it is possible that the Wnt/PCP pathway, like its *Drosophila* counterpart, is involved in the regulation of cell polarity during vertebrate gastrulation. However, while in the *Drosophila* wing epithelium the ultimate readout of planar cell polarisation is the unidirectional (monopolar) orientation of one wing hair per cell, no equivalent Wnt/PCP-dependent monopolar cell polarisation has been observed during vertebrate gastrulation.

In this study, we analysed the role of *slb/wnt11* in regulating cell movements and morphology during zebrafish gastrulation. From 3D reconstruction and motion analysis of individual cells, we present evidence that *slb/wnt11* is required for the directionality and velocity of movements of hypoblast cells in the forming germ ring at the onset of gastrulation. We further demonstrate that *slb* hypoblast cells that have impaired migratory cell movements also exhibit defects in the orientation of cellular processes along their individual movement directions. This indicates that process orientation mediated by *slb/wnt11* is crucial for facilitating and stabilising hypoblast cell movements at the onset of gastrulation. These observations provide the first direct evidence of a role of the *slb/wnt11* signalling pathway in regulating process orientation and migratory cell movements at early stages of zebrafish gastrulation.

Materials and methods

Staging and maintenance of embryos

All zebrafish strains were maintained as described (Heisenberg et al., 1996). Wild-type embryos were taken from AB, gol*, TL and Tübingen backgrounds. Embryos from homozygous slb^{tx226} carriers were used for mutant analysis. Transgenic *gsc*GFP embryos were produced in the TL background as previously described (Gilmour et al., 2002).

In situ hybridisation and gelatine sectioning

Whole-mount in situ hybridisation was performed as previously described (Barth and Wilson, 1995). For sections, in situ-stained embryos were equilibrated in gelatine/albumen solution (0.49% gelatine, 30% egg albumen, 20% sucrose in PBS), transferred into an embedding form coated with fresh polymerisation solution (albumen, 25% glutaraldehyde, 10:1) and kept 15 minutes at room temperature to allow polymerisation. 20-μm serial sections were taken using a Leica Vibratome VT1000S.

mRNA misexpression

For ubiquitous overexpression, mRNA was injected into the yolk of zygote/one-cell stage embryos as previously described (Barth and Wilson, 1995). For scatter labelling of wild-type and *slb* mutant embryos, a mixture of 30-100 pg cytosolic GFP mRNA and 60-150 pg GAP43-GFP mRNA was injected into single blastomeres of 8-32-cell stage embryos. Transgenic gscGFP embryos were scatter labelled by injecting 250 pL of 0.5% rhodamine-dextrane with M_r=2.000×10^3 (Molecular Probes, Eugene) in 0.2 M KCl into single blastomeres of embryos at the 8- to 32-cell stage.

Confocal imaging

Shield-stage embryos were manually dechorionated and mounted in 1% agarose in E3 fish medium. Life images were obtained at room temperature with a 60×water-immersion objective on a BioRad Radiance 2000 Multiphoton Confocal Microscope setup.

For dual channel confocal timelapses, 488 nm Ar Laser and 543 nm He/Ne laser lines were used simultaneously. The emitted light passed through a 560 nm dichroic mirror/long path filter. Image z-stacks were obtained by scanning areas of 204.8 μm×204.8 μm (0.4 μm pixel^{-1}) with 166 lines per second and 1.5 μm steps over a total vertical distance of 66 μm. For each experiment, 12-20 image stacks were acquired in 4-minute time intervals.

For single channel timelapse recordings, z-stacks were acquired by scanning an area of 102.4 μm×102.4 μm (0.2 μm pixel^{-1}) with 750 lines second^{-1} and 0.5 μm steps over a total vertical distance of 50 μm. Stacks were taken continuously with no time gap in between. A mode-locked infrared laser line between 890 and 910 nm with an average power of 500 mW was used, originating from a Mira 900 two-photon Ti::Sapphire laser. A 532 nm laser source with 5 W output power was used as a pump laser (Coherent, California).

Image analysis

The acquired confocal z-stacks were volume rendered in 3D over time using the program Volocity (Improvision, UK). The cell movement analysis was also carried out using this software by manually measuring the positions of the geometric centre of the cells (the cell centroid) in three dimensions. Tracing was done manually by outlining the cell borders, using a newly developed version of the 3D-DIAS software (Soll et al., 2000; Heid et al., 2002). The cell bodies were always traced separately from cellular processes. Every cellular extension that emerged from the cell body at an angle of <135° and

a width of >2 μm was defined as a pseudopodial extension. Epiblast and prechordal plate precursor cells were identified according to their position and net movement direction. The cell traces were rendered in three dimensions and measured using newly developed JAVA-based 3D-DIAS software (E.V. and D.R.S., unpublished), which allowed the quantification of several morphometric parameters such as the surface area, volume, centroid position and roundness ($rnd=6\times V\times\pi^{0.5}\times A^{-1.5}$) of single cells in three dimensions.

The subsequent analysis of the obtained morphological data was carried out using Microsoft Excel and ProFit (Quantum Soft, Basel). To account for the resolution limit in z-direction and because the manual traces could not always be perfect, processes that had <5% of the length of the corresponding cell body, were <2 μm long or had a volume $<1.25\times10^{-2}$% and a roundness >0.7 were not analysed.

Statistical analysis

Student's *t*-test (Microsoft Excel) with a two-tailed distribution was used to analyse significance between two mean values. For analysis of correlation between process orientation and movement persistence, a special Microsoft Excel plug-in was used that tested a linear dependence between the parameters (Müller et al., 2002).

Results

slb/wnt11 is expressed in epiblast cells of the germ ring

To obtain insight into the cellular function of *slb/wnt11*, we first determined the expression domains of *slb/wnt11* in wild-type embryos at the onset of gastrulation. *slb/wnt11* is expressed around the circumference of the germ ring with slightly reduced expression at the region of the forming shield (organiser) (Fig. 1A) (Makita et al., 1998). Within the germ ring, *slb/wnt11* was expressed predominantly in epiblast cells (ectodermal germ layer), whereas ingressing hypoblast cells (mesendodermal germ layer) showed no detectable levels of *slb/wnt11* expression (Fig. 1B-D). This indicates that *slb/wnt11*, expressed in epiblast cells, might be involved in the control of cell movements in the germ ring that mediate ingression of hypoblast cells at the onset of gastrulation.

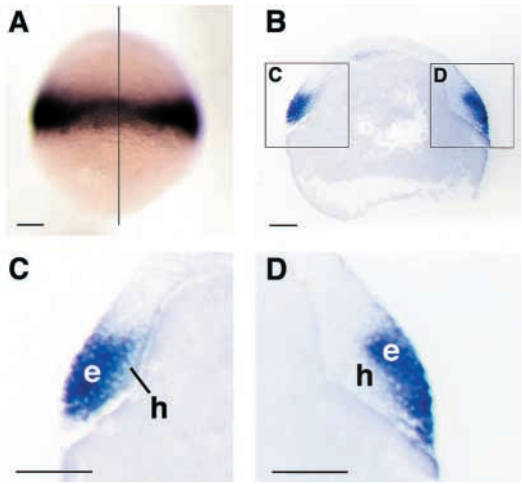

Fig. 1. *slb/wnt11* is expressed in epiblast cells (ectoderm) overlying the first ingressing hypoblast cells (mesendoderm) at the germ ring during early stages of gastrulation. (A) Dorsal view of *slb/wnt11* expression in the germ ring of a wild-type embryo at shield stage. The vertical line indicates the section plane shown in B-D. (B-D) Medial section of the embryo in A showing *slb/wnt11* expression in epiblast cells (B). The boxed regions are shown at higher magnification in C (ventral germ ring) and D (shield). e, epiblast; h, hypoblast. Scale bars: 100 μm.

slb prechordal plate cells show slower and less directed movements

To examine if *slb/wnt11* was required for the movements of ingressing hypoblast cells at early stages of gastrulation, we determined the positions and shapes of axial mesendodermal tissues, such as the prechordal plate and notochord, in wild-type and *slb*-mutant embryos at different timepoints throughout the onset of gastrulation. In wild-type embryos, the prechordal plate moved rapidly anteriorly from the shield towards the animal pole during the first 2-3 hours of gastrulation (Fig. 2A-D), whereas in *slb* mutants, this movement appeared to be reduced 45 minutes after the onset of gastrulation (Fig. 2E-H). A similar reduction in anterior cell movement was also observed in paraxial mesendodermal tissues of *slb* embryos (data not shown). These early cell-movement defects are unlikely to be caused by secondary variations in the genetic background because they were at least partially rescued by ubiquitous overexpression of *wnt11* mRNA in *slb* mutants (Fig. 2I-L).

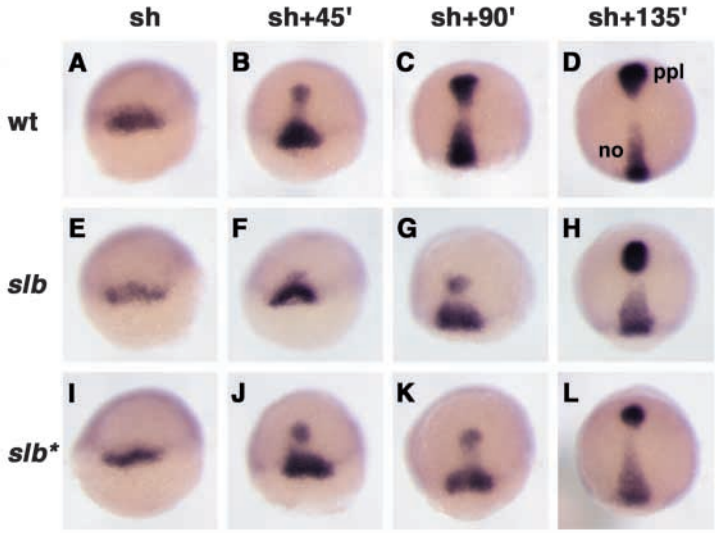

Fig. 2. Extension of axial mesendodermal tissues (prechordal plate and notochord) is reduced in *slb* embryos throughout the early stages of gastrulation. Embryos were fixed at various times after shield stage (sh) and stained for the expression of *hatching gland gene 1* (*hgg1*) and *floating head* (*flh*) to mark the positions of the prechordal plate (ppl) and the notochord (no), respectively. (A-L) Shape and position of prechordal plate and notochord in wild-type embryos (wt, A-D), *slb* mutants (*slb*, E-H) and *slb* mutants overexpressing 5 pg *slb/wnt11* mRNA (*slb**, I-L) at the indicated time intervals. For each experiment and timepoint, 20 embryos were analysed. Anterior to the top, dorsal views.

To obtain a more dynamic image of prechordal plate morphogenesis in wild-type and *slb* mutant embryos at the onset of gastrulation, we analysed the movement of individual cells in the axial hypoblast (presumptive prechordal plate) and overlying epiblast (ectoderm). Using confocal timelapse imaging, we simultaneously recorded the positions of

prechordal plate precursor cells that expressed green fluorescent protein (GFP) in the cytosol under the control of the goosecoid (gsc) promotor (see Movie 1 at http://dev.biologists.org/supplemental/), and of overlying epiblast cells labelled with rhodamine-dextrane (red). These timelapse sequences revealed that most hypoblast and epiblast cells in wild-type embryos move parallel to the surface of the yolk sac in a straight path towards the animal pole and germ ring, respectively (Fig. 3A-E; see Movie 2 at http://dev.biologists.org/supplemental/). By contrast, corresponding hypoblast cells of *slb* mutants have less directed movements parallel to the surface of the yolk sac and increased movements along the dorso-ventral and medio-lateral axes (Fig. 3F-J; see Movie 3 at http://dev.biologists.org/supplemental/).

To quantify the differences between the cell movements in wild type and *slb* embryos, we calculated the average persistence (the shortest distance between the start and end points of the movement divided by the total distance moved, in percent) as an expression of how 'straight' or 'direct' a cell moves, and the velocity (in $\mu m\ min^{-1}$) of these movements in 3D between shield stage and 75% epiboly (140 minutes). In total, we recorded 30 epiblast cells and 20 hypoblast cells, using two wild-type and two *slb* embryos. Both the average velocity and persistence of cell movements within the hypoblast were reduced significantly in *slb* mutants compared to wild-type controls (1.24±0.23 $\mu m\ min^{-1}$ in wild type versus 1.06±0.22 $\mu m\ min^{-1}$ in *slb* mutants, $P=9.4\times10^{-4}$; and 84.35±6.52% in wild type versus 37.54±20.77% in *slb* mutants, $P=7.63\times10^{-18}$). By contrast, the velocity and persistence of epiblast cell movements in *slb* mutants are indistinguishable from wild-type controls (data not shown). This indicates that *slb/wnt11* controls the velocity and persistence of hypoblast, but not epiblast, cell movements at the onset of gastrulation.

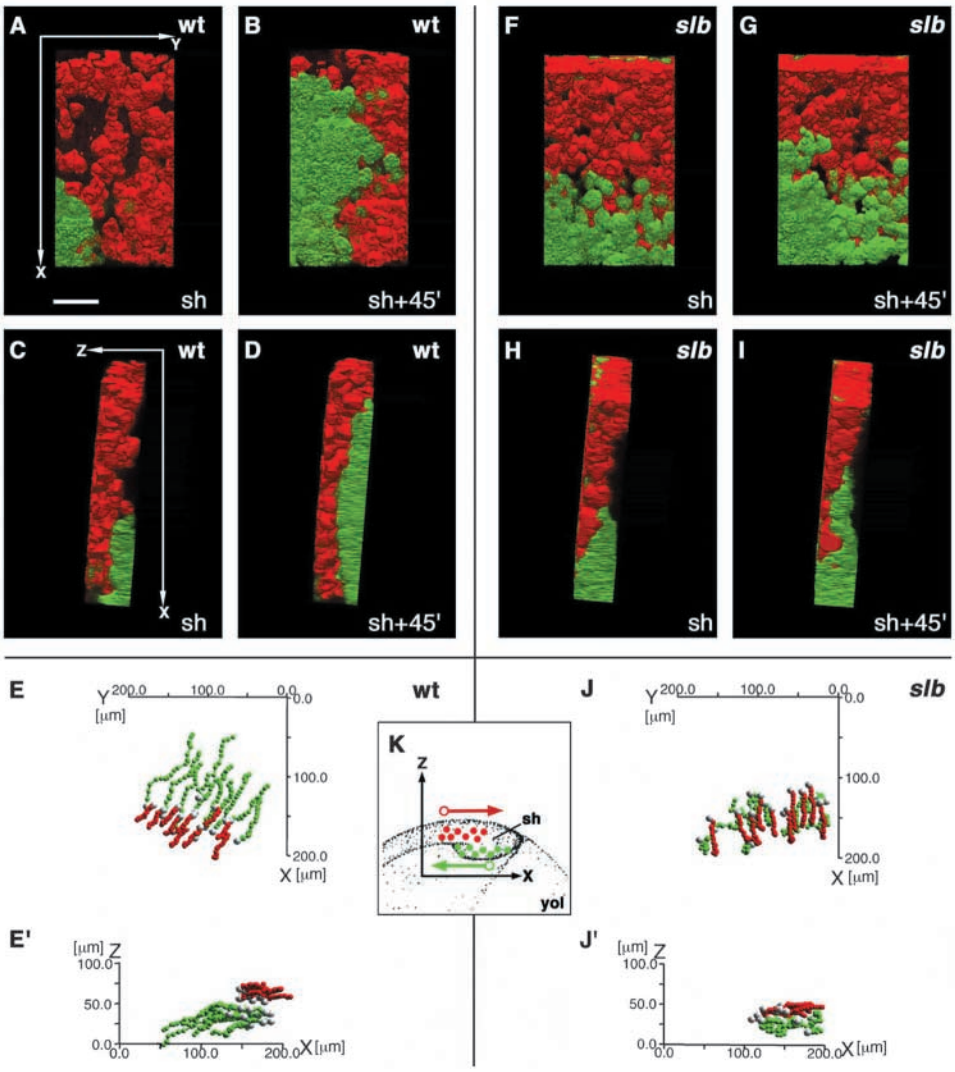

Fig. 3. Movement of axial hypoblast (presumptive prechordal plate) cells in dorsal regions of the germ ring (shield) is disturbed in *slb* mutant embryos at the onset of gastrulation. Embryos expressing GFP (green) under the control of the *goosecoid* (*gsc*) promotor in prechordal plate precursor cells were scatter labelled with rhodamine (red) in epiblast cells overlying the presumptive prechordal plate and followed in 3D over time by dual channel confocal microscopy. (A-D,F-I) Prechordal plate precursor cells (green) and overlying epiblast cells (red) in wild-type (A-D) and *slb* (F-I) *gsc*GFP embryos at shield stage (A,C,F,H) and 45 minutes (45′) later (B,D,G,I). Ventral views (A,B,F,G) and lateral views with ventral to the right and dorsal to the left (C,D,H,I). In all pictures, anterior is to the top and posterior to the bottom. The axes of orientation are shown in panels A and C. (E,E′,J,J′) Track diagrams showing the movements of prechordal plate precursor cells (green) and epiblast cells (red) in wild type (E,E′) and *slb* *gsc*GFP embryos (J,J′) along the x (anterior-posterior) and y (medio-lateral) axes (E,J) and along the x and z (dorsal-ventral) axes (E′,J′) of the embryo. The positions of the geometric centre of the cell (the centroid) were measured in 3D at 4-minute intervals and plotted as a single dot. Each line represents the track of one cell, with the first timepoint depicted in white. The net movement of the epiblast cells is along the +x (posterior) direction and that of prechordal plate precursor cells along the –x (anterior) direction. Note that the x, y and z axes depict the global coordinates within the gastrula, whereas in Figs 4, 5 and 7, these axes show the coordinates relative to the movement direction of individual cells. (K) Schematic diagram showing the orientation of the region analyzed in wild-type and *slb* embryos and the net movement direction of the cells (arrows) with respect to the x and z axes. The y axis is perpendicular to x and z and is not depicted in this diagram. Epiblast cells in red, hypoblast cells in green. Note that a left-handed coordinate system has been used. sh, shield; yol, yolk. Scale bar in A: 50 μm.

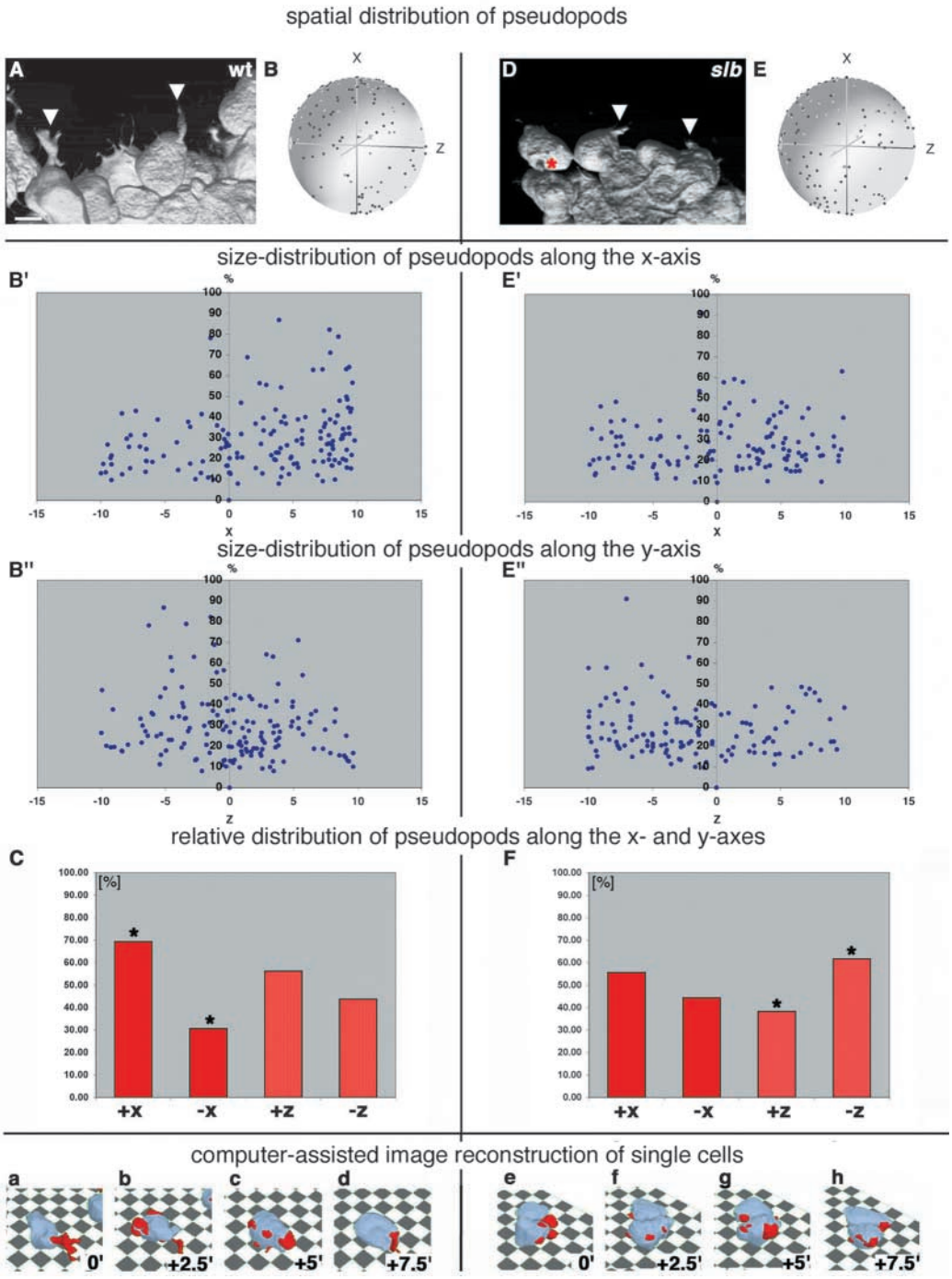

Fig. 4. Distribution of pseudopodial processes in wild-type and *slb* prechordal plate precursor cells at the onset of gastrulation. Prechordal plate precursor cells were labelled with a mixture of cytosolic and membrane-bound GFP and visualised in 3D over time by two-photon confocal microscopy. (A,D) 3D images of prechordal-plate-precursor cells in a wild-type (A) and *slb* mutant embryo (D) moving from bottom (germ ring margin) to top (animal pole) at shield stage. Arrowheads point to thick, pseudopod-like processes and the red asterisk (D) marks a pseudopod projecting into the dorsal direction. (B,E) Spherical plots showing the distribution of the outgrowth positions of pseudopods (blue dots) relative to the cell centroid and normalized to the movement direction of the cells (black dot) in wild-type (B) and *slb* mutant (E) embryos at shield stage. For these spherical diagrams, the 3D distribution of the positions where pseudopods emerged on the surface of each cell (blue dots) was measured relative to the centroid of the cell body. The position of the centroid for the succeeding timepoint was also measured. The distances between the positions of the pseudopod and the cell centroid were then calibrated to a constant value, leaving the orientation of the pseudopod positions unchanged. Plotted in 3D with the cell centroid at the origin, the pseudopod positions were, thus, placed at the surface of a sphere centred around the origin. These spherical graphs were then turned so that the positions of each cell centroid for the following timepoint (black dot) were placed onto the x-axis. The pseudopod positions in 20 cells from five wild-type and five *slb* embryos at four consecutive timepoints (0, 2.5, 5 and 7.5 minutes) were plotted into one diagram. To enhance the 3D appearance of the plots, an artificial transparent sphere centred at the origin was added to each diagram. Note that the x, y and z axes in these diagrams show the coordinates relative to the movement direction of individual cells (+x axis), whereas in Fig. 3, these axes depict the global coordinates within the gastrula. (B′,E′) Distribution of pseudopod lengths from B and E, respectively, along the x-axis. (B′,E′) – the individual movement axis of the cells – or the z-axis (B″,E″). Each diagram shows pseudopod lengths relative to the body length of the corresponding cell (in %); the numbers on the ordinate axis correspond to arbitrary units, with x=10 being the radius of the spheres in (B) and (E). (C,F) Distribution of the outgrowth positions of pseudopods in wild-type (C) and *slb* mutant (F) embryos. The columns show the relative distribution of pseudopods along (+x versus –x) or perpendicular (+z versus –z) to the individual movement direction of the cells, averaged over four consecutive timepoints (0, 2.5, 5 and 7.5 minutes), with the cell centroid at x=0 and z=0. The insets show examples of wild-type (a-d) and *slb* (e-h) prechordal plate cells after 3D reconstruction with the software used to quantify the data, with cell body and pseudopods in light blue and red, respectively. The corresponding timepoints are indicated. *, $P<0.05$, paired Student's *t*-test. Scale bar in A: 10 μm.

slb mesendodermal cells exhibit defects in the orientation of their cellular processes along their individual movement directions

To investigate the cellular mechanisms that underlie the cell-movement defects in *slb* mutants, we recorded the morphology of individual cells labelled with a mixture of cytosolic and membrane-anchored GFP (Okada et al., 1999) using two-photon confocal microscopy. Parameters of cell morphology, such as the number, shape and orientation of cellular processes, were measured in 3D over time. Process orientation was calculated relative to the individual movement direction of each cell by determining the points on the cell surface where processes emerged. Temporal changes in the morphology of cellular processes were quantified by calculating the total length and roundness, which measures how efficiently a surface encloses a volume (Heid et al., 2002), of each process at different timepoints (see Materials and methods).

First, we analysed the morphology of axial hypoblast cells at the leading edge of the presumptive prechordal plate. We chose those cells because they have more distinct processes than cells in more posterior parts of the prechordal plate (data not shown) and are, therefore, easier to analyse in respect to process formation and orientation. By analysing dynamic changes in the orientation of cellular processes relative to changes in the movement directions of single cells, we found that wild-type prechordal-plate precursor cells form pseudopod-like processes (average roundness <0.7) that are oriented preferentially towards their individual directions of movement (+x axis, Fig. 4A-C; see Movie 4 at http://dev.biologists.org/supplemental/; average percentage of processes per cell in +x versus –x direction at all timepoints, 70% versus 30%; s.d., 38%; P=1.6×10^{-5}). By contrast, these cells show no such process orientation in *slb* mutant embryos (Fig. 4D-F and data not shown), but preferentially orient their processes towards the underlying cells or substrate (–z direction; Fig. 4D-F; see Movie 4 at http://dev.biologists.org/supplemental/; average percentage of processes per cell in +z versus –z direction over all timepoints, 39% versus 61%; s.d., 39%; P=9.0×10^{-3}). Comparison of the dynamic changes in the distribution of pseudopod lengths between wild-type and *slb* hypoblast cells along the x and z axes indicates that most elongated processes point into the +x direction in wild-type embryos but not in *slb* mutants (Fig. 4B′,B″,E′,E″). The average number, shape and length of processes revealed no obvious differences between wild type and *slb* hypoblast cells (data not shown).

We also analysed the morphology of single epiblast cells that were either in front of or directly above the first ingressing prechordal-plate-precursor cells in wild type and *slb* mutant embryos. Wild-type epiblast cells formed pseudopod-like processes (average roundness <0.7) that were oriented towards and away from their individual movement directions (+x direction). However, we were unable to detect statistically significant differences in the distribution of these processes along the x axis (Fig. 5A-C and data not shown; see Movie 5 at http://dev.biologists.org/supplemental/), indicating that pseudopod-like processes in wild-type epiblast cells are not oriented preferentially towards their individual movement directions. Similarly, *slb* epiblast cells showed no preferential orientation of their processes towards their individual movement directions (Fig. 5D-F and data not shown). However, unlike wild-type epiblast cells, they formed processes that were oriented preferentially towards the underlying cells or substrate (–z direction; Fig. 5D-F; Movie 5 at http://dev.biologists.org/supplemental/; average percentage of processes per cell in +z versus –z direction at all timepoints, 36% versus 64%; s.d., 36%; P, 3.1×10^{-3}). Comparison of the distribution of pseudopod lengths along the x and z axes and the average number, shape and length of processes in wild-type and *slb* epiblast cells revealed no obvious differences (Fig. 5B′,B″,E′,E″ and data not shown).

To complement our study on cellular processes, we also analysed dynamic changes of different morphometric parameters that describe the shape of the cell body (excluding processes), such as surface area, volume, and cell elongation, in hypoblast and epiblast cells from wild-type and *slb* mutant embryos. However, we detected no significant differences in any of these parameters between wild type and mutant embryos (data not shown), which indicates that *slb/wnt11* is not required for the general shape of the cell body itself in hypoblast and epiblast cells at the onset of gastrulation.

Taken together, these findings indicate that *slb/wnt11* is needed in hypoblast cells to orient pseudopod-like processes towards their individual movement directions. In the absence of *slb/wnt11* activity, both hypoblast and epiblast cells reorient their processes towards the underlying cells or substrate. The requirement for *slb/wnt11* appears to be specific to process orientation, because the general shape of the cell body in epiblast and hypoblast cells is unchanged in *slb* mutants.

The *slb* mesendodermal cell morphology defect is linked to less directed movements of these cells and can be rescued by ubiquitous overexpression of *slb/wnt11*

To investigate if the change in the preferential orientation of cellular processes in *slb* mutant cells was linked to the cell movement defect in these cells, we determined the movement persistence of individual hypoblast cells (Fig. 3 and see above) in relation to the percentage of processes oriented towards their individual movement directions in wild-type and *slb* mutant embryos. Wild-type hypoblast cells that have processes preferentially oriented towards their individual movement directions also show highly persistent movements, whereas in *slb* mutant cells, a reduction in the percentage of processes oriented towards their individual movement directions is accompanied by less persistent movements (Fig. 6). Testing the correlation between process orientation and movement persistence for all cells analysed (wild type and *slb*) shows that these values are statistically linked (P=0.02; r=0.36) (Müller et al., 2002). This indicates that *slb/wnt11*-mediated orientation of cellular processes is needed in hypoblast cells for the directionality of cell movements at the onset of gastrulation.

To further confirm that the defective process orientation in *slb* hypoblast cells is specifically caused by the absence of *slb/wnt11* function, we ubiquitously overexpressed *slb/wnt11* mRNA in *slb* mutant embryos and determined the orientation of cellular processes in hypoblast cells at the onset of gastrulation. We conducted the morphometric analysis in two dimensions (x-y plane), because this allowed us to analyse a larger number of cells than is possible using equivalent 3D representations. At the onset of gastrulation, hypoblast cells from *slb* mutant embryos overexpressing 5 pg of *slb/wnt11*

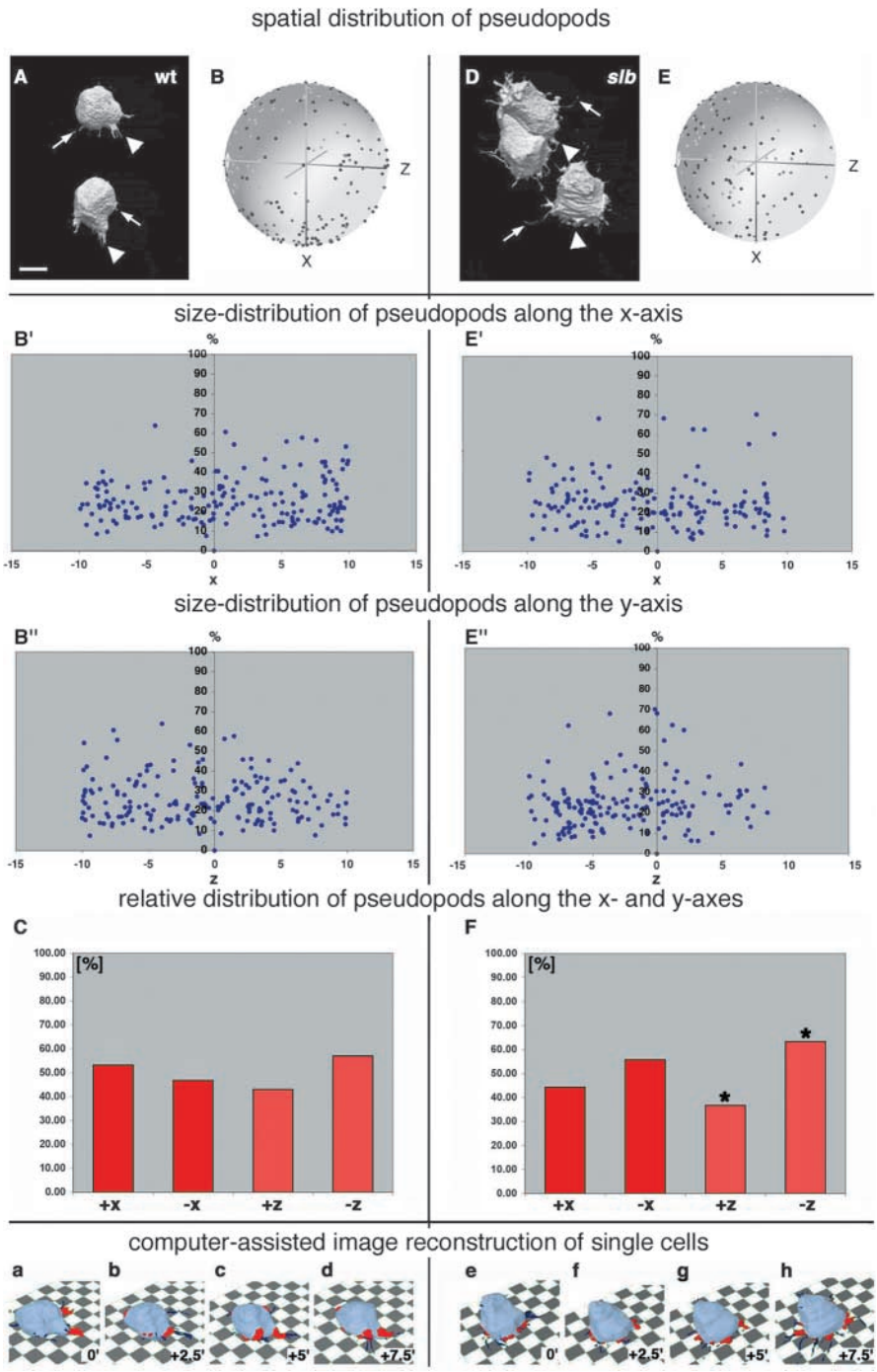

Fig. 5. Distribution of processes in wild-type and *slb* epiblast cells overlying the presumptive prechordal plate at the onset of gastrulation. Cells were labelled with a mixture of cytosolic and membrane-bound GFP and visualised in 3D over time by two-photon confocal microscopy. (A,D) 3D images of typical epiblast cells in a wild-type (A) and *slb* mutant (D) embryo moving from top (animal pole) to bottom (germ ring margin) at shield stage. Arrowheads point to thick, pseudopod-like processes. Arrows mark smaller, filopod-like processes. In A, the pseudopod emerging from the upper cell is branched. (B,E) Spherical plots showing the distribution of the outgrowth positions of pseudopods (blue dots) relative to the cell centroid and normalized to the movement direction of the cells (black dot) in wild-type (B) and *slb* mutant (E) embryos at shield stage (see Fig. 4 for further information on spherical plots). The process positions of 20 cells (from four timepoints in wild type and the first three timepoints in *slb*) or from 11 cells (last timepoint in *slb*) from five wild-type and eight *slb* embryos at four consecutive timepoints (0, 2.5, 5 and 7.5 minutes) were plotted into one diagram. Note that the x, y and z axes in these diagrams show the coordinates relative to the movement direction of individual cells (+x axis), whereas in Fig. 3, these axes depict the global coordinates within the gastrula. (B′,B′′,E′,E′′) Distribution of pseudopod lengths from B and E, respectively, along the x-axis (B′,E′) – the individual movement axis of the cells – or the z-axis (B′′,E′′). Each diagram shows pseudopod lengths relative to the body length of the corresponding cell (in %); the numbers on the ordinate axis correspond to arbitrary units, with x=10 being the radius of the spheres in (B) and (E). (C,F) Distribution of the outgrowth positions of pseudopods in wild-type (C) and *slb* embryos (F). The columns show the relative distribution of pseudopods along (+x versus –x) and perpendicular (+z versus –z) to the individual movement direction of the cells, averaged over four consecutive timepoints (0, 2.5, 5 and 7.5 minutes), with the cell centroid at x=0 and z=0. The insets show examples of wild-type (a-d) and *slb* (e-h) epiblast cells, with cell bodies in light blue and pseudopods in red. The corresponding timepoints are indicated. The dark blue structures are thin, filopod-like processes. *, $P<0.05$, paired Student's *t*-test. Scale bar in A: 10 μm.

mRNA per embryo preferentially orient their pseudopod-like processes towards their individual movement directions. This is similar to but slightly weaker than in equivalent wild-type cells (87% versus 13% in +x versus –x direction, s.d.=13%, $P=7.4\times10^{-6}$ in wild-type cells; 61% versus 39% in +x versus –x direction, s.d.=12%, $P=0.04$ in *slb* cells overexpressing *slb/wnt11*). By contrast, no preferential orientation was detected in cells from uninjected *slb* mutants (57% versus 43% in +x versus –x direction, s.d.=22%, $P=0.29$). This rescue of the process-orientation phenotype in hypoblast cells from *slb/wnt11* overexpressing embryos is even more pronounced at mid-gastrulation stages (Fig. 7A,C,D; 90% versus 10% in +x versus –x direction, s.d.=12%, $P=8.11\times10^{-10}$ in *slb* cells overexpressing *slb/wnt11*; 87% versus 13%, s.d.=15%, $P=2.11\times10^{-7}$ in wild-type cells). By contrast, hypoblast cells from uninjected *slb* embryos at mid-gastrulation have a significantly lower preferential orientation of their processes (Fig. 7B,D; 66% versus 34%, s.d.=21%, $P=3.78\times10^{-3}$) when

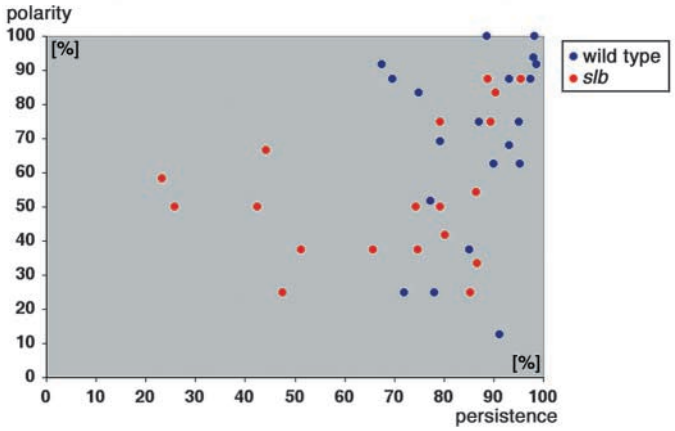

Fig. 6. Scatter plot of the relationship between the orientation of hypoblast cell processes towards their individual movement directions (y-axis with % of processes in movement direction) in relation to the degree of persistence of their movements (x-axis), determined for five consecutive timepoints (0, 2.5, 5, 7.5 and 10 minutes) in 20 wild type (blue-dots) and 20 *slb* cells (red dots) from five embryos each.

compared to wild type (P=2.9×10^{-3}) and *slb/wnt11*-overexpressing *slb* cells (P=3.5×10^{-4}). Taken together, these results indicate that ubiquitous overexpression of *slb/wnt11* can rescue the hypoblast process orientation phenotype in *slb* mutant embryos during early stages of gastrulation.

Discussion

In this study, we have analysed the cellular function of *slb/wnt11* in the forming germ ring at the onset of gastrulation. We found that *slb/wnt11* is required for the orientation of cellular processes in hypoblast cells towards their individual movement directions and that the aberrant orientation of cellular processes in *slb* mutant hypoblast cells is accompanied by slower, less directed migratory cell movements. We conclude that *slb/wnt11* is needed for the orientation of cellular processes in hypoblast cells and that the correct orientation of cellular processes in these cells facilitates and stabilises their movements.

The cellular function of *slb/wnt11* at the onset of gastrulation

The main finding of this study is that *slb/wnt11* is required for both cellular process orientation and directed cell movements of hypoblast cells at the onset of gastrulation. To obtain insight into the relationship of process orientation and cell movement in single cells, we developed an assay that allows us to compare dynamic changes in process orientation with changes in the direction of cell movements. We showed that in wild-type hypoblast cells, process orientation and movement direction are aligned, whereas in *slb* mutant cells, no such alignment is observed. The misalignment of process orientation and movement direction in *slb* mutants is linked to less efficient movements of hypoblast cells towards the animal pole. However, although these cells move slower with more frequent changes in the movement direction ('less persistent movement'), the net direction of their movement appears to be unaffected. This indicates that the role of *slb/wnt11*-mediated orientation of cellular processes in the direction of individual cell movements is to facilitate and stabilise these movements, rather than to determine the overall direction of movement.

How do these findings relate to previous studies that implicate *slb/wnt11* and the Wnt/PCP pathway in the regulation of CE movements at later stages of gastrulation (reviewed by Tada et al., 2002; Wallingford et al., 2002)? We analysed the function of *slb/wnt11* in cells that were morphogenetically distinct from cells undergoing CE movements. Hypoblast cells in the region of the forming germ ring at the onset of gastrulation do not show medio-lateral cell intercalation behaviour nor elongate along their medio-lateral axes (M.L.C. and C.P.H., unpublished), as described for cells undergoing CE movements (Concha and Adams, 1998; Glickman et al., 2003). Instead, they move as loosely

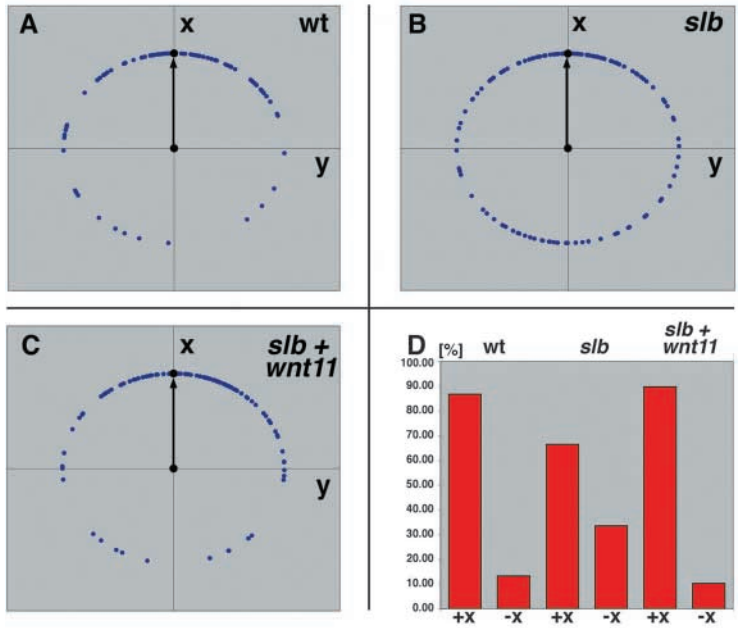

Fig. 7. Two-dimensional distribution of pseudopodial processes in wild-type, *slb* and *slb/wnt11* injected *slb* prechordal plate precursor cells at midgastrulation stages. As in Figs 4 and 5, cells were labelled with a mixture of cytosolic and membrane-bound GFP and visualised over time by two-photon confocal microscopy. (A-C) Polar plots of the distribution of the outgrowth positions of pseudopods (blue dots) relative to the cell centroid and normalized to the movement direction of the cells (black arrows) in wild-type (A), *slb* (B) and *slb* embryos injected with 5 pg *slb/wnt11* mRNA (C) at 75% epiboly. These polar plots were made similar to the spherical plots shown in Figs 4 and 5 (see above), except that the outgrowth positions of the pseudopods and the cell centroids were originally determined in two dimensions. For each genotype, the process positions in 5-10 cells over 5-15 consecutive timepoints (4-minute time intervals) from two embryos were analysed and plotted into one diagram. Note that the x and y axes show the coordinates relative to the movement direction of individual cells (+x direction) and do not resemble the global coordinates within the gastrula. (D) Relative distribution of the outgrowth positions of pseudopods (in %) along the individual movement direction of the cells (+x and –x) in wild-type and *slb* embryos and *slb* embryos injected with 5 pg *slb/wnt11* mRNA, averaged over all timepoints analysed.

associated cells in a straight path towards the animal pole, similar to the behaviour of cells with directed migration on a substrate [this study and Warga and Kimmel (Warga and Kimmel, 1990)]. Consequently, we found that *slb/wnt11* is required for the orientation of cellular processes along the movement axis of individual cells, a feature that is associated commonly with migrating cells in vitro and in vivo (Lauffenburger and Horwitz, 1996).

By contrast, the cellular functions of the Wnt/PCP pathway in controlling cell movements during CE have not been fully addressed. Reduced medio-lateral cell elongation in different mutant and morphant phenotypes of the Wnt/PCP pathway has been associated with slower, less persistent cell movements at late stages of gastrulation (Darken et al., 2002; Goto and Keller, 2002; Jessen et al., 2002; Marlow et al., 2002; Park and Moon, 2002; Topczewski et al., 2001; Wallingford et al., 2000). However, the specific changes in cell elongation have not been correlated with the dynamic changes in the individual movement directions of these cells. Moreover, these cells have been analysed mainly in two dimensions (x-y plane). This limits the view on those cells and, consequently, the interpretation of these observations because cells undergoing CE movements can also exhibit distinctive movements along the z-axis (Glickman et al., 2003) (F.U. and C.P.H., unpublished). Future studies to compare the role of the Wnt/PCP pathway in cellular dynamics during early versus late stages of gastrulation are needed to reveal the common and divergent aspects of Wnt/PCP signalling during the course of gastrulation.

Potential target processes of *slb/wnt11* at the onset of gastrulation

How does *slb/wnt11* control the orientation of cellular processes and directed cell movements in the germ ring at the onset of gastrulation? Our observation that *slb/wnt11* is expressed within the epiblast, although it is required predominantly in the hypoblast, indicates that *slb/wnt11*, produced in epiblast cells, directly or indirectly influences hypoblast cell movement and morphology. It is possible that *slb/wnt11*, secreted by epiblast cells, might exert direct control over hypoblast cell morphogenesis by regulating rearrangements of the hypoblast cytoskeleton that control the formation and orientation of processes in these cells. *slb/wnt11* might function either permissively, by allowing these cells to extend and stabilise cellular processes in their preferred orientation, or it might function instructively, by determining the orientation of these processes. Our observation that ubiquitous overexpression of *slb/wnt11* rescued the cell morphology and movement phenotype of *slb* mutants argues in favour of a more permissive function of *slb/wnt11* in this process. Findings from recent studies in zebrafish, which show that Rok2, which directly regulates cytoskeletal elements such as myosin in *Drosophila*, is a downstream component of the *slb/wnt11* signalling pathway support a function of *slb/wnt11* in regulating cytoskeletal dynamics (Marlow et al., 2002).

Alternatively, *slb/wnt11* might also indirectly affect morphogenesis of hypoblast tissue by regulating the differential adhesiveness of hypoblast and epiblast cells, which would have a secondary effect on process orientation and directed cell movement. The finding that hypoblast (and epiblast) cells in *slb* mutants reorient their processes towards the underlying cell(s) or the yolk-cell surface indicates that, in the absence of *slb/wnt11* function, either the adhesion of these cells to their respective substrates is increased or adhesion between these cells is decreased. Indeed, our own preliminary observations show that *slb* hypoblast cells in culture display a reduced tendency to ‘cluster’ (F.U. and C.P.H., unpublished), which indicates that there are defects in cell-cell or cell-substrate adhesion. Further support for a role of *slb/wnt11* in regulating cell adhesion comes from recent studies in *Xenopus*, which show that the presumptive receptor for Wnt11, Fz7, is required for the effective separation of mesoderm from ectoderm at the onset of gastrulation (Winklbauer et al., 2001).

It is likely that *slb/wnt11* uses both of these, and possibly other unknown, processes to control cellular morphology and movements during gastrulation. Future studies should identify the specific requirements of these target processes for the function of *slb/wnt11* in different tissues during the course of gastrulation.

We thank Jennifer Geiger, Mathias Köppen, Christian Dahmann and Marcos Gonzalez-Gaitan for helpful comments on earlier versions of this manuscript, Beate Kilian for technical assistance, Ugur Yalcin, Katrin Anczok and Viktor Schnabel for help with the image analysis, Vinzenz Link for programming Excel Macros and Harald Brush-Janovjak for extensive reviews of the statistics part of this work. We are grateful to Kurt Anderson and Jan Peychl for help with the confocal microscopy. P.J.H., E.V. and D.R.S. are supported by NIH grant HD-18577, The W.M Keck Foundation and the Developmental Studies Hybridoma Bank (DSHB), P.J.H. by The American Cancer Society (grant # PF-01-110-01-CSM), M.L.C. and S.W.W. by the Wellcome Trust, M.T. by an MRC Career Development Award, and F.U. and C.P.H. by an Emmy-Noether-Fellowship from the DFG.

References

Adler, P. N. (2002). Planar signaling and morphogenesis in Drosophila. *Dev. Cell* **2**, 525-535.

Barth, K. A. and Wilson, S. W. (1995). Expression of zebrafish nk2.2 is influenced by sonic hedgehog/vertebrate hedgehog-1 and demarcates a zone of neuronal differentiation in the embryonic forebrain. *Development* **121**, 1755-1768.

Concha, M. L. and Adams, R. J. (1998). Oriented cell divisions and cellular morphogenesis in the zebrafish gastrula and neurula: a time-lapse analysis. *Development* **125**, 983-994.

Darken, R. S., Scola, A. M., Rakeman, A. S., Das, G., Mlodzik, M. and Wilson, P. A. (2002). The planar polarity gene strabismus regulates convergent extension movements in Xenopus. *EMBO J.* **21**, 976-985.

Djiane, A., Riou, J., Umbhauer, M., Boucaut, J. and Shi, D. (2000). Role of frizzled 7 in the regulation of convergent extension movements during gastrulation in Xenopus laevis. *Development* **127**, 3091-3100.

Elul, T. and Keller, R. (2000). Monopolar protrusive activity: a new morphogenic cell behavior in the neural plate dependent on vertical interactions with the mesoderm in Xenopus. *Dev. Biol.* **224**, 3-19.

Elul, T., Koehl, M. A. and Keller, R. (1997). Cellular mechanism underlying neural convergent extension in Xenopus laevis embryos. *Developmental Biology (Orlando)* **191**, 243-258.

Gilmour, D. T., Maischein, H. M. and Nüsslein-Volhard, C. (2002). Migration and function of a glial subtype in the vertebrate peripheral nervous system. *Neuron* **34**, 577-588.

Glickman, N. S., Kimmel, C. B., Jones, M. A. and Adams, R. J. (2003). Shaping the zebrafish notochord. *Development* **130**, 873-887.

Goto, T. and Keller, R. (2002). The planar cell polarity gene strabismus regulates convergence and extension and neural fold closure in Xenopus. *Dev. Biol.* **247**, 165-181.

Habas, R., Dawid, I. B. and He, X. (2003). Coactivation of Rac and Rho by Wnt/Frizzled signaling is required for vertebrate gastrulation. *Genes Dev.* **17**, 295-309.

Habas, R., Kato, Y. and He, X. (2001). Wnt/Frizzled activation of rho

regulates vertebrate gastrulation and requires a novel formin homology protein daam1. *Cell* **107**, 843-854.

Hammerschmidt, M., Pelegri, F., Mullins, M. C., Kane, D. A., Brand, M., van Eeden, F. J., Furutani-Seiki, M., Granato, M., Haffter, P., Heisenberg, C. P. et al. (1996). Mutations affecting morphogenesis during gastrulation and tail formation in the zebrafish, *Danio rerio*. *Development* **123**, 143-151.

Hannus, M., Feiguin, F., Heisenberg, C. P. and Eaton, S. (2002). Planar cell polarization requires Widerborst, a B′ regulatory subunit of protein phosphatase 2A. *Development* **129**, 3493-3503.

Heid, P. J., Voss, E. and Soll, D. R. (2002). 3D-DIASemb: a computer-assisted system for reconstructing and motion analyzing in 4D every cell and nucleus in a developing embryo. *Dev. Biol.* **245**, 329-347.

Heisenberg, C. P., Brand, M., Jiang, Y. J., Warga, R. M., Beuchle, D., van Eeden, F. J., Furutani-Seiki, M., Granato, M., Haffter, P., Hammerschmidt, M. et al. (1996). Genes involved in forebrain development in the zebrafish, Danio rerio. *Development* **123**, 191-203.

Heisenberg, C. P. and Nüsslein-Volhard, C. (1997). The function of silberblick in the positioning of the eye anlage in the zebrafish embryo. *Developmental Biology (Orlando)* **184**, 85-94.

Heisenberg, C. P., Tada, M., Rauch, G. J., Saude, L., Concha, M. L., Geisler, R., Stemple, D. L., Smith, J. C. and Wilson, S. W. (2000). Silberblick/Wnt11 mediates convergent extension movements during zebrafish gastrulation. *Nature* **405**, 76-81.

Jessen, J. R., Topczewski, J., Bingham, S., Sepich, D. S., Marlow, F., Chandrasekhar, A. and Solnica-Krezel, L. (2002). Zebrafish *trilobite* identifies new roles for Strabismus in gastrulation and neuronal movements. *Nat. Cell Biol.* **4**, 610-615.

Keller, R. (2002). Shaping the vertebrate body plan by polarised embryonic cell movements. *Science* **298**, 1950-1954.

Keller, R. and Danilchik, M. (1988). Regional expression, pattern and timing of convergence and extension during gastrulation of Xenopus laevis. *Development* **103**, 193-209.

Keller, R. and Tibbetts, P. (1989). Mediolateral cell intercalation in the dorsal, axial mesoderm of Xenopus laevis. *Developmental Biology (Orlando)* **131**, 539-549.

Keller, R. E., Danilchik, M., Gimlich, R. and Shih, J. (1985). The function and mechanism of convergent extension during gastrulation of Xenopus laevis. *Journal of Embryology & Experimental Morphology* **89** Suppl. 185-209.

Keller, R., Shih, J. and Domingo, C. (1992). The patterning and functioning of protrusive activity during convergence and extension of the Xenopus organiser. *Development Suppl.* 81-91.

Keller, R., Davidson, L., Edlund, A., Elul, T., Ezin, M., Shook, D. and Skoglund, P. (2000). Mechanisms of convergence and extension by cell intercalation. *Philos. Trans. R. Soc. Lond. B Biol. Sci.* **355**, 897-922.

Kilian, B., Mansukoski, H., Barbosa, F. C., Ulrich, F., Tada, M. and Heisenberg, C. P. (2003). The role of Ppt/Wnt5 in regulating cell shape and movement during zebrafish gastrulation. *Mech. Dev.* **120**, 467-476.

Lauffenburger, D. A. and Horwitz, A. F. (1996). Cell migration: a physically integrated molecular process. *Cell* **84**, 359-369.

Makita, R., Mizuno, T., Koshida, S., Kuroiwa, A. and Takeda, H. (1998). Zebrafish Wnt11 – Pattern and regulation of the expression by the yolk cell and no tail activity. *Mech. Dev.* **71**, 165-176.

Marlow, F., Topczewski, J., Sepich, D. and Solnica-Krezel, L. (2002). Zebrafish rho kinase 2 acts downstream of wnt11 to mediate cell polarity and effective convergence and extension movements. *Curr. Biol.* **12**, 876-884.

Muller, P. Y., Janovjak, H., Miserez, A. R. and Dobbie, Z. (2002). Processing of gene expression data generated by quantitative real-time RT-PCR. *Biotechniques* **32**, 1372-1379.

Okada, A., Lansford, R., Weimann, J. M., Fraser, S. E. and McConnell, S. K. (1999). Imaging cells in the developing nervous system with retrovirus expressing modified green fluorescent protein. *Exp. Neurol.* **156**, 394-406.

Park, M. and Moon, R. T. (2002). The planar cell-polarity gene stbm regulates cell behaviour and cell fate in vertebrate embryos. *Nat. Cell Biol.* **4**, 20-25.

Rauch, G. J., Hammerschmidt, M., Blader, P., Schauerte, H. E., Strahle, U., Ingham, P. W., McMahon, A. P. and Haffter, P. (1997). Wnt5 is required for tail formation in the zebrafish embryo. *Cold Spring Harbor Symposia on Quantitative Biology* **62**, 227-234.

Shih, J. and Keller, R. (1992). Cell motility driving mediolateral intercalation in explants of Xenopus laevis. *Development* **116**, 901-914.

Soll, D. R., Voss, E., Johnson, O. and Wessels, D. (2000). Three-dimensional reconstruction and motion analysis of living, crawling cells. *Scanning* **22**, 249-257.

Solnica-Krezel, L., Stemple, D. L., Mountcastle-Shah, E., Rangini, Z., Neuhauss, S. C., Malicki, J., Schier, A. F., Stainier, D. Y., Zwartkruis, F., Abdelilah, S. et al. (1996). Mutations affecting cell fates and cellular rearrangements during gastrulation in zebrafish. *Development* **123**, 67-80.

Strutt, D. I. (2002). The asymmetric subcellular localisation of components of the planar polarity pathway. *Semin. Cell Dev. Biol.* **13**, 225-231.

Sumanas, S. and Ekker, S. C. (2001). Xenopus frizzled-7 morphant displays defects in dorsoventral patterning and convergent extension movements during gastrulation. *Genesis* **30**, 119-122.

Sumanas, S., Kim, H. J., Hermanson, S. and Ekker, S. C. (2001). Zebrafish frizzled-2 morphant displays defects in body axis elongation. *Genesis* **30**, 114-118.

Tada, M., Concha, M. L. and Heisenberg, C. P. (2002). Non-canonical Wnt signalling and regulation of gastrulation movements. *Semin. Cell Dev. Biol.* **13**, 251-260.

Topczewski, J., Sepich, D. S., Myers, D. C., Walker, C., Amores, A., Lele, Z., Hammerschmidt, M., Postlethwait, J. and Solnica-Krezel, L. (2001). The zebrafish glypican knypek controls cell polarity during gastrulation movements of convergent extension. *Dev. Cell* **1**, 251-264.

Wallingford, J. B., Rowning, B. A., Vogeli, K. M., Rothbacher, U., Fraser, S. E. and Harland, R. M. (2000). Dishevelled controls cell polarity during *Xenopus* gastrulation. *Nature* **405**, 81-85.

Wallingford, J. B., Fraser, S. E. and Harland, R. M. (2002). Convergent extension: the molecular control of polarized cell movement during embryonic development. *Dev. Cell* **2**, 695-706.

Warga, R. M. and Kimmel, C. B. (1990). Cell movements during epiboly and gastrulation in zebrafish. *Development* **108**, 569-580.

Winklbauer, R., Medina, A., Swain, R. K. and Steinbeisser, H. (2001). Frizzled-7 signalling controls tissue separation during *Xenopus* gastrulation. *Nature* **413**, 856-860.